2022 American Control Conference (ACC)
Atlanta, USA, June 8-10, 2022

Distributed and Resilient Planning-Control for Optimal LEO Satellite Constellation Coverage

Yuhan Zhao and Quanyan Zhu

Abstract— **Coverage services provided by LEO satellite constellations have served as the base platform for various space applications. However, the surge of space attacks such as physical and cyber attacks are greatly endangering the security of satellite constellations and the integrity of the coverage services. As repairs of satellites are challenging, a distributed protection mechanism is necessary to ensure the self-healing of the satellite constellation coverage from different attacks. To this end, this paper establishes a distributed framework to empower a resilient satellite constellation coverage design and control within a single orbit. Each satellite can make decisions individually to recover from adversarial and non-adversarial attacks and keep providing coverage service. We first provide the average coverage cost to measure the coverage performance. Then, we formulate the joint resilient coverage planning-control problem as a two-stage problem by decoupling the coverage planning and fuel-optimal control. A distributed algorithm is proposed to find the optimal coverage configuration. The multi-waypoint MPC methodology is adopted to steer satellites to the target configuration. Finally, we use a typical LEO satellite constellation as a case study to corroborate the results.**

I. Introduction

Recent advances in space technology research and development have inspired numerous applications of Low Earth Orbit (LEO) satellite constellations, such as positioning [1], communications [2], and remote sensing [3]. Among various research and applications, satellite constellation coverage plays a fundamental role, where multiple LEO satellites work cooperatively to provide global or regional coverage service [4]–[6]. As the satellite constellation coverage serves as the platform for other space applications such as space-terrestrial internet and TV signal transmission, one of the challenges in LEO constellation design and control is maintaining a good coverage performance. Apart from the classical approaches to design global coverage [7], [8] and regional coverage [9], recent research such as [10]–[12] have also studied the optimal satellite deployment to maximize joint coverage.

However, the booming security threats in the space domain make the satellites more vulnerable during the operation and degenerate the coverage performance. For example, physical attacks [13] such as laser attacks can directly destroy satellite entities. Cyber attacks such as jamming [14], [15] can block and disrupt satellite signals, causing degeneration or failure to the coverage service. Apart from the adversarial attacks, non-adversarial threats such as orbit debris can also put satellites at risk and harm the coverage service. It is estimated in [16] that there have been more than one hundred satellite attacks, including jamming and hijacking, since 1977, many of which have caused a significant loss in navigation and communication. Therefore, we need reliable mechanisms to protect satellite constellations and improve the resiliency of satellite constellation coverage for various attacks.

Resiliency ensures the survivability of satellite constellations under successful attacks. It also provides flexibility and adaptability to cope with security threats. However, few works have focused on resiliency in the space domain although it has been studied in other fields such as [17], [18]. Besides, centralized approaches for optimal LEO satellite constellation design such as [5], [12] are insufficient to address the security challenges for the following reasons. First, most constellation designs do not consider satellite control, making it harder for constellation recovery and adjustment because satellite repair and replenishment can be challenging. Second, not all satellites can connect to the same central station simultaneously because they scatter in space, which brings further difficulties for satellite coordination.

To this end, we develop a distributed framework that enables a resilient satellite constellation coverage planning and control in a single orbit under adversarial and non-adversarial attacks. We first propose the average coverage cost to measure the coverage performance of the single-orbit satellite constellation by using the notion of the satellite configuration. Next, we formulate an optimal planning-control problem that jointly optimizes the coverage performance and the fuel consumption for satellite constellation self-healing. We further take advantage of the distributed nature of the satellite constellation and reformulate the planning-control problem to a two-stage problem, i.e., the planning and the control stages. At the planning stage, we propose a distributed algorithm to find optimal coverage deployment under both adversarial and non-adversarial attacks. At the control stage, we use multi-waypoint Model Predictive Control to achieve autonomous self-healing control. We also use a case study to demonstrate that our distributed framework provides resiliency to the satellite constellation coverage problem.

The rest of the paper is organized as follows. Section II introduces the preliminary for satellite control and constellation measurement. Section III formulates the satellite constellation planning-control problem. We propose a distributed coverage planning algorithm in Section IV and synthesize our distributed planning-control framework in Section V. Case studies on a typical LEO constellation are presented in Section VI, and Section VII concludes the paper.

This work is partially supported by grants SES-1541164, ECCS-1847056, CNS-2027884, and BCS-2122060 from National Science Foundation (NSF), grant 20-19829 from DOE-NE, and grant W911NF-19-1-0041 from Army Research Office (ARO). The authors are with the Department of Electrical and Computer Engineering, New York University. Emails: {yhzhao, qz494}@nyu.edu.

II. Preliminary

A. Clohessy-Wiltshire Equations for Satellite Control

Due to small orbit eccentricity, LEO satellites rotate in nearly circular orbits. For satellite S_i, we attach a moving frame S_i-xyz called the *local vertical local horizontal* (LVLH) frame shown in Fig. 1, where S_i is the *chief location*, x-axis points outward along the radial direction, y-axis points to the velocity direction, and z-axis is perpendicular to the orbital plane. Due to the nonlinearity, the *relative motion* [19]—the satellite motion described in the LVLH frame—is in general used to describe the satellite dynamics and is captured by the Clohessy-Wiltshire (CW) equations [20]:

$$\delta\ddot{x} - 3\omega^2\delta x - 2\omega\delta\dot{y} = 0, \tag{1}$$

$$\delta\ddot{y} + 2\omega\delta\dot{x} = 0, \tag{2}$$

$$\delta\ddot{z} + \omega^2\delta z = 0, \tag{3}$$

where ω is the mean motion and $(\delta x, \delta y, \delta z) \in \mathbb{R}^3$ are the displacements in the LVLH frame. The last equation (3) indicates that the relative motion along z-axis is independent from the one in xy-plane. We assume that the satellite does not switch the orbit plane during the operation and ignore (3) for satellite control. Let $p_i = [p_{ix}\ p_{iy}]^\mathsf{T} \in \mathbb{R}^2$ and $v_i = [v_{ix}\ v_{iy}]^\mathsf{T} \in \mathbb{R}^2$ be the relative position and relative velocity in xy-plane of the LVLH frame respectively, and $u_i = [u_{ix}\ u_{iy}]^\mathsf{T} \in \mathbb{R}^2$ be the control thrust. We have

$$\begin{bmatrix}\dot{p}_i \\ \dot{v}_i\end{bmatrix} = \begin{bmatrix}0 & 0 & 1 & 0 \\ 0 & 0 & 0 & 1 \\ 3\omega^2 & 0 & 0 & 2\omega \\ 0 & 0 & -2\omega & 0\end{bmatrix}\begin{bmatrix}p_i \\ v_i\end{bmatrix} + \begin{bmatrix}0_{2\times 1} \\ u_i\end{bmatrix} := A\begin{bmatrix}p_i \\ v_i\end{bmatrix} + Bu_i, \tag{4}$$

When satellite S_i moves to the relative position p_i, it also forms a deviation angle $\Delta\phi_i(p_i)$ with x-axis shown in Fig. 1. Let r_s be the orbital radius. Using geometry, we can compute

$$\Delta\phi_i(p_i) = \operatorname{sgn}(p_{iy}) \arccos\left(\frac{p_{ix} + r_s}{\sqrt{(p_{ix} + r_s)^2 + p_{iy}^2}}\right). \tag{5}$$

B. Satellite Configuration

We consider n satellites rotating in the same circular orbit with orbital radius r_s and mean motion ω (period $T_s = \frac{2\pi}{\omega}$). We denote the i-th satellite as S_i and the index increasing direction is the same as the satellite moving direction.

Definition 1. *A satellite configuration (or configuration) of n LEO satellites in the same orbit refers to a stable passive formation such that the relative position between any two satellites remains constant.*

To measure a satellite configuration, we introduce the geocentric polar frame O-L shown in Fig. 1, which is fixed on the earth surface. Then we define the configuration angle.

Definition 2. *The configuration angle ϕ_i for satellite S_i is the angle between x-axis of the LVLH frame and OL axis. The initial configuration angle (ICA) ϕ_i^0 corresponds to the initial configuration (IC) at time $\tau = 0$.*

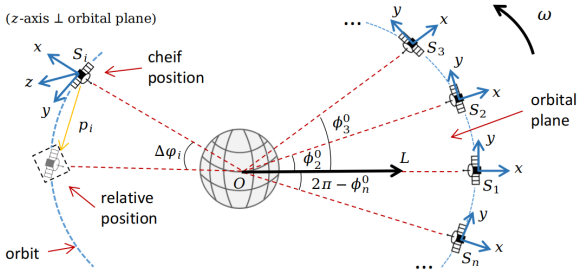

Fig. 1: [left-half] The LVLH frame on Satellite S_i. [right-half] Satellite configuration at time $\tau = 0$.

For any IC, we define $\phi_1^0 = 0$ and $\Delta\phi_i(0) = 0$ for all $i = 1, \ldots, n$. Since all satellites are not stationary to the earth, ϕ_i changes with time τ and the relative position p_i:

$$\phi_i(p_i, \tau) = \phi_i^0 + \Delta\phi_i(p_i) + \omega\tau, \quad i = 1, \ldots, n. \tag{6}$$

Given an IC, any new configuration can be characterized the relative position vector $\mathbf{p} = [p_1^\mathsf{T}\ \cdots\ p_n^\mathsf{T}]^\mathsf{T} \in \mathbb{R}^{2n}$.

III. Problem Setting

In this section, we first introduce the coverage performance measure of the satellite constellation and then formulate the coverage planning-control problem as a two-stage problem.

A. Metric for Coverage Performance

Once all n satellites form a configuration, they start to provide coverage services. Let $\mu : \mathbb{R} \to \mathbb{R}$ be the global demand intensity on the orbit ground track measured in O-L frame. Due to the fast velocity of LEO satellites, we assume that μ is time-invariant. We extend $\mu(\theta)$ to a periodic function with period 2π for computational purposes, i.e., $\mu(\theta) = \mu(\theta + 2k\pi)$, $k \in \mathbb{Z}$. At time τ, satellite S_i covers part of the earth surface shown in Fig. 2. Let α_i be the coverage angle, which is determined by the field of view (FOV) angle with the coverage geometry. We denote C_i as the coverage region and assume symmetric coverage to the ground. Then we write $C_i := C_i(p_i, \tau) = C_i^+ \cup C_i^- \cup \{\phi_i(p_i, \tau)\}$, where

$$\begin{aligned} C_i^+ &:= (\phi_i(p_i, \tau), \phi_i(p_i, \tau) + \alpha_i), \\ C_i^- &:= (\phi_i(p_i, \tau) - \alpha_i, \phi_i(p_i, \tau)). \end{aligned} \tag{7}$$

Note that C_i may overlap with C_j $(j \neq i)$ to ensure that the ground is fully covered. We define $\mathcal{N}_i$ as set of satellites which share the overlapped coverage region with satellite S_i. Due to the ring structure of the satellite configuration, we only consider the adjacent neighbors, i.e., $\mathcal{N}_i = \{S_{i-1}, S_{i+1}\}$[1]. We use linear coverage intensity for satellite S_i in C_i. Let ψ_i^{m} be the maximum coverage intensity and $k_i := \psi_i^{\mathrm{m}}/\alpha_i$, the *local coverage intensity* is defined by

$$\psi_i(\theta, p_i, \tau) = \begin{cases} -k_i(\theta - \omega\tau - \Delta\phi_i(p_i) - \phi_i^0) + \psi_i^{\mathrm{m}} & \theta \in C_i^+ \cup \{\phi_i\} \\ k_i(\theta - \omega\tau - \Delta\phi_i(p_i) - \phi_i^0) + \psi_i^{\mathrm{m}} & \theta \in C_i^- \\ 0 & \text{o.w.} \end{cases} \tag{8}$$

To measure the overall configuration coverage, we define the *global coverage intensity function* $\rho(\theta, \mathbf{p}, \tau) =$

[1]For clarity, satellite S_{n+1} refers to S_1 and satellite S_0 refers to S_n.

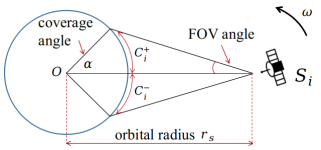

Fig. 2: Coverage geometry of a single satellite.

$\sum_{i=1}^{n} \psi_i(\theta, p_i, \tau)$. A good configuration should meet the coverage demand as much as possible. Therefore, the average supply-demand intensity difference is an indicator to measure the coverage performance. Taking the periodicity into consideration, we define the *average coverage cost* $J : \mathbb{R}^{2n} \to \mathbb{R}$ for a configuration

$$J(\mathbf{p}) = \frac{1}{2T_s} \int_{\tau=0}^{T_s} \int_{\theta=\omega\tau}^{\omega\tau+2\pi} \|\rho(\theta, \mathbf{p}, \tau) - \mu(\theta)\|_2^2 \, \mathrm{d}\theta \mathrm{d}\tau. \tag{9}$$

A smaller $J(\mathbf{p})$ indicates a better coverage performance.

B. Two-Stage Problem Formulation

When encountering adversarial or non-adversarial attacks, some satellites' coverage capabilities can be affected. The current configuration may no longer be optimal to provide the coverage service. Therefore, we formulate a two-stage problem, i.e., the planning and control stages, as a resilient and distributed architecture to (a) improve the resiliency of the satellite constellation to adapt to insecure environments and (b) take the satellite's limited fuel supply for maneuver into consideration.

The planning stage problem seeks a configuration that minimizes the coverage cost when the current configuration is no longer optimal. Since the configuration is characterized by the relative position vector, we seek a vector $\mathbf{p}$ such that

$$\begin{aligned} \min_{\mathbf{p}} \quad & J(\mathbf{p}) \\ \text{s.t.} \quad & (p_{ix} + r_s)^2 + p_{iy}^2 = r_s^2, \quad i = 1, \dots, n. \end{aligned} \tag{$\mathcal{Q}_p$}$$

The constraints indicate that all satellites should remain in the same orbit when the new configuration is found. This is because changing the orbit can break the configuration and makes it harder for satellite controls. It also increases the probability of colliding with satellites in other orbits.

The planning stage problem ($\mathcal{Q}_p$) outputs the target configuration $\mathbf{p}^{\mathrm{d}}$ to adapt to new attacks. The control stage problem steers all satellites to $\mathbf{p}^{\mathrm{d}}$ by minimizing the fuel consumption (measured by the total control cost). Let p_i^{d} be the i-th component of $\mathbf{p}^{\mathrm{d}}$. Due to independent dynamics (4), each satellite can autonomously drive to the target position by its own fuel-optimal controls. For satellite S_i, the control stage problem can be formulated as

$$\begin{aligned} \min_{u_i} \quad & \frac{1}{2} \int_{t=0}^{T_f} \left(\|u_i\|_{R_i}^2 + \|v_i\|_{Q_i}^2 \right) \mathrm{d}t \\ \text{s.t.} \quad & \begin{bmatrix} \dot{p}_i \\ \dot{v}_i \end{bmatrix} = A \begin{bmatrix} p_i \\ v_i \end{bmatrix} + B u_i, \quad \|u_i(t)\|_2 \le u_i^{\mathrm{m}}, \\ & p_i(T_f) = p_i^{\mathrm{d}}, \quad v_i(T_f) = 0. \end{aligned} \tag{$\mathcal{Q}_{ci}$}$$

The terminal constraints require that all satellites indeed form the desired stable configuration after the control.

In the following sections, we suppress function arguments for simplicity. For example, ρ stands for $\rho(\theta, \mathbf{p}, \tau)$.

IV. Distributed Coverage Planning and Analysis

In this section, we introduce a distributed algorithm for satellite constellation coverage planning. We also provide the analysis of the target configuration found by our algorithm.

A. Distributed Structure of Coverage Measure

Despite the coupling in the coverage cost J, we can utilize the configuration structure to design distributed algorithms to find the local minimum. For satellite S_i, from (8) we have

$$\frac{\partial \psi_i}{\partial p_i} = \begin{cases} k_i \begin{bmatrix} \frac{-p_{iy}}{(p_{ix}+r_s)^2+p_{iy}^2} & \frac{p_{ix}+r_s}{(p_{ix}+r_s)^2+p_{iy}^2} \end{bmatrix} & \theta \in C_i^+ \cup \{\phi_i\} \\ -k_i \begin{bmatrix} \frac{-p_{iy}}{(p_{ix}+r_s)^2+p_{iy}^2} & \frac{p_{ix}+r_s}{(p_{ix}+r_s)^2+p_{iy}^2} \end{bmatrix} & \theta \in C_i^- \\ 0 & \text{o.w.} \end{cases} \tag{10}$$

Following the definition of ρ, we have

$$\begin{aligned} \frac{\partial J}{\partial p_i} &= \frac{1}{2T_s} \int_{\tau=0}^{T_s} \int_{C_i} 2(\rho - \mu) \frac{\partial \psi_i}{\partial p_i} \mathrm{d}\theta \mathrm{d}\tau \\ &= \frac{1}{T_s} \int_{\tau=0}^{T_s} \int_{C_i} \rho \frac{\partial \psi_i}{\partial p_i} \mathrm{d}\theta \mathrm{d}\tau - \frac{1}{T_s} \int_{\tau=0}^{T_s} \int_{C_i} \mu \frac{\partial \psi_i}{\partial p_i} \mathrm{d}\theta \mathrm{d}\tau. \end{aligned} \tag{11}$$

The ring structure of the configuration indicates that satellite S_i only needs to communicate with its neighbors to compute $\frac{\partial J}{\partial p_i}$. With the assumption of the time-invariant demand μ, we can further simplify (11) with the following lemma.

Lemma 1. *Let $f : \mathbb{R} \to \mathbb{R}$ be a function with $f(x) \ge 0$ and $f(x) = f(x + T)$. For any $\delta \in [0, T)$, the function $G(x) = F(x + \delta) - F(x)$ is periodic with period T, where $F(x) = \int f(x) \mathrm{d}x$. Hence $\int_0^T G(x) \mathrm{d}x = \int_0^T G(x + \epsilon) \mathrm{d}x$ for any $\epsilon \in \mathbb{R}$.*

Using Lemma 1, we arrive at the following proposition.

Proposition 1. *The integral $\frac{1}{T_s} \int_0^{T_s} \int_{C_i} \mu \frac{\partial \psi_i}{\partial p_i} \mathrm{d}\theta \mathrm{d}\tau$ in (11) is equal to 0 for all satellite S_i, $i = 1, \dots, n$.*

Proof. The proof can be found in [21]. □

With Prop. 1, (11) becomes

$$\frac{\partial J}{\partial p_i} = \frac{1}{T_s} \int_0^{T_s} \int_{C_i} \rho \frac{\partial \psi_i}{\partial p_i} \mathrm{d}\theta \mathrm{d}\tau. \tag{12}$$

Based on (12), we can design distributed gradient descent (GD) methods for all satellites to jointly solve for ($\mathcal{Q}_p$).

B. Distributed Projected Gradient Descent Algorithm

The constraints in ($\mathcal{Q}_p$) indicate that all the satellites stay in the same orbit during the operation. We use projected gradient descent methods to find the local optimum of ($\mathcal{Q}_p$). Let $\Omega_i = \{p_i | (p_{ix} + r_s)^2 + p_{iy}^2 = r_s^2\}$. The iteration follows

$$p_i^{(k+1)} = \mathrm{proj}_{\Omega_i} \left(p_i^{(k)} - s^{(k)} \frac{J^{(k)}}{\partial p_i} \right),$$

where (k) denotes the k-th iteration, $s^{(k)}$ is the step size, and $\mathrm{proj}_{\Omega_i}(\cdot)$ is the projection operator. Since Ω_i are independent, we propose the distributed projected gradient descent (DPGD) algorithm for coverage planning in Alg.1.

When some satellite S_i reach the condition $\frac{\partial J}{\partial p_i} = 0$, it does not implies that satellite S_i terminates the algorithm.

The influence from other satellites can propagate to S_i and perturb its gradient. We use a counter cnt_i to ensure the gradient remains small enough for some time (lines 15-21).

Algorithm 1: DPGD for coverage planning.

1 **Initialize**: $p_i^{(0)}, \mathrm{exit}_i^{(0)} \leftarrow$ false, $\mathrm{cnt}_i \leftarrow 0$ for all S_i ;
2 Activate satellite set $\mathcal{S}_A \leftarrow \{S_1, S_2, \ldots, S_n\}$;
3 All S_i broadcast and receive (α_i, ψ_i^m) ;
4 $k \leftarrow 0$; // global iteration for DPGD
5 **while** $\mathcal{S}_A \neq \varnothing$ **do**
6 **for** *Satellite* $S_i \in \mathcal{S}_A$ *(parallel)* **do**
7 Broadcast $p_i^{(k)}, \mathrm{exit}_i^{(k)}$ to $S_j \in \mathcal{N}_i$;
8 Receive $p_j^{(k)}, \mathrm{exit}_j^{(k)}$ from $S_j \in \mathcal{N}_i$;
9 **for** $S_j \in \mathcal{N}_i$ **do**
10 **if** $\mathrm{exit}_j^{(k)}$ **then**
11 $p_j^{(k+1)} \leftarrow p_j^{(k)}$, $\mathrm{exit}_j^{(k+1)} \leftarrow$ true;
12 Identify $C_i^{(k)}$ with $(\alpha_j, \psi_j^m, p_j^{(k)})$, $j \in \mathcal{N}_i$;
13 Compute $\frac{\partial J^{(k)}}{\partial p_i}$ with (12) ;
14 **if** $\left\|\partial J^{(k)}/\partial p_i\right\| < \epsilon_i$ **then**
15 $\mathrm{cnt}_i \leftarrow \mathrm{cnt}_i + 1$;
16 $p_i^{(k+1)} \leftarrow p_i^{(k)}$;
17 **else**
18 $\mathrm{cnt}_i \leftarrow 0$;
19 $p_i^{(k+1)} = \mathrm{proj}_{\Omega_i}\left(p_i^{(k)} - s^{(k)} \frac{J^{(k)}}{\partial p_i}\right)$;
20 **if** $\mathrm{cnt}_i > \max\_\mathrm{cnt}$ **or** $k > \max\_\mathrm{k}$ **then**
21 $\mathrm{exit}_i^{(k+1)} \leftarrow$ true ;
22 $\mathcal{S}_A \leftarrow \mathcal{S}_A \backslash \{S_i\}$;
23 $k \leftarrow k + 1$;

C. Analysis of Stationary Point

When the convergence is guaranteed, the DPGD algorithm Alg. 1 generates a stationary point $\mathbf{p}^*$ for $(\mathcal{Q}_p)$. Since the projection is involved at $\mathbf{p}^*$, we must have[2] either $\frac{\partial J^*}{\partial p_i} = 0$ or $\frac{\partial J^*}{\partial p_i}$ parallel to x-axis of the LVLH frame for $i = 1, \ldots, n$. However, the latter case can be ruled out by (10) because $\frac{\partial \psi_i}{\partial p_i}$ is never parallel to x-axis of the LVLH frame. Therefore, at any stationary point $\mathbf{p}^*$ generated by Alg. 1, we have

$$\int_0^{T_s} \int_{C_i^+} \rho \mathrm{d}\theta \mathrm{d}\tau = \int_0^{T_s} \int_{C_i^-} \rho \mathrm{d}\theta \mathrm{d}\tau, \quad i = 1, \ldots, n. \tag{13}$$

Next, we show that the stationary point $\mathbf{p}^*$ is the local minimum under certain conditions. We discuss the scenario where every satellite shares overlapping coverage regions with its adjacent neighbors. i.e, C_i overlaps both with C_{i+1} and C_{i-1} for $i = 1, \ldots, n$. From (12), we have

$$\frac{\partial^2 J}{\partial p_i^2} = \frac{1}{T_s} \int_0^{T_s} \int_{C_i} \left(\frac{\partial \psi_i}{\partial p_i}\right)^{\mathsf{T}} \frac{\partial \psi_i}{\partial p_i} + \rho \frac{\partial^2 \psi}{\partial p_i^2} \mathrm{d}\theta \mathrm{d}\tau.$$

We can compute $\frac{\partial^2 \psi_i}{\partial p_i^2}$ from (10). By referring to the stationary condition (13), at $\mathbf{p}^*$ we have

$$\frac{1}{T_s} \int_0^{T_s} \int_{C_i} \rho^* \frac{\partial^2 \psi_i^*}{\partial p_i^2} \mathrm{d}\theta \mathrm{d}\tau = 0, \quad i = 1, \ldots, n,$$

[2]We write $J^* = J(\mathbf{p}^*)$ for simplicity.

where $\rho^* := \rho(\theta, \mathbf{p}^*, \tau)$ and $\psi_i^* := \psi_i(\theta, \mathbf{p}^*, \tau)$. Therefore,

$$\frac{\partial^2 J^*}{\partial p_i^2} = \frac{2\alpha_i k_i^2}{[(p_{ix}^* + r_s)^2 + p_{iy}^{*2}]^2} \begin{bmatrix} -p_{iy}^* \\ p_{ix}^* + r_s \end{bmatrix} \begin{bmatrix} -p_{iy}^* & p_{ix}^* + r_s \end{bmatrix}.$$

We also note that $\frac{\partial}{\partial p_j} \frac{\partial \psi_i}{\partial p_i} = 0$ for $j \neq i$. Hence

$$\frac{\partial^2 J}{\partial p_i \partial p_j} = \frac{1}{T_s} \int_0^{T_s} \int_{\omega\tau}^{\omega\tau + 2\pi} \left(\frac{\partial \psi_j}{\partial p_j}\right)^{\mathsf{T}} \frac{\partial \psi_i}{\partial p_i} \mathrm{d}\theta \mathrm{d}\tau.$$

From (8), we see that $\frac{\partial^2 J}{\partial p_i \partial p_j} \neq 0$ if and only if S_i and S_j share an overlapped coverage region. Since only adjacent neighbors are considered, for satellite S_i, we have

$$\begin{aligned} \frac{\partial^2 J}{\partial p_i \partial p_{i+1}} &= \frac{1}{T_s} \int_0^{T_s} \int_{C_i \cap C_{i+1}} \left(\frac{\partial \psi_{i+1}}{\partial p_{i+1}}\right)^{\mathsf{T}} \frac{\partial \psi_i}{\partial p_i} \mathrm{d}\theta \mathrm{d}\tau \\ &= \left(\frac{\partial \psi_{i+1}}{\partial p_{i+1}}\right)^{\mathsf{T}} \frac{\partial \psi_i}{\partial p_i} (\phi_i - \phi_{i+1} + \alpha_i + \alpha_{i+1}). \end{aligned}$$

Likewise,

$$\frac{\partial^2 J}{\partial p_i \partial p_{i-1}} = \left(\frac{\partial \psi_{i-1}}{\partial p_{i-1}}\right)^{\mathsf{T}} \frac{\partial \psi_i}{\partial p_i} (\phi_{i-1} - \phi_i + \alpha_i + \alpha_{i-1}).$$

Therefore, the Hessian $\frac{\partial^2 J}{\partial \mathbf{p}^2}$ has a banded structure and we have the following proposition to characterize the property of the stationary point $\mathbf{p}^*$.

Proposition 2. *Let $\mathbf{p}^*$ be the stationary point generated by the DPGD algorithm. $\mathbf{p}^*$ is a local minimum of J if $\left|\phi_i^0 - \phi_{i+1}^0 + \Delta\phi_i - \Delta\phi_{i+1} + \alpha_i + \alpha_{i+1}\right| \leq \sqrt{\alpha_i \alpha_{i+1}}$ for all $i = 1, 2, \ldots, n-1$. For $i = n$, the term $\phi_n^0 - \phi_1^0$ is changed to $2\pi - \phi_n^0 + \phi_1^0$ due to periodicity.*

Proof. The proof can be found in [21]. □

The condition in Prop. 2 indicates that for any two adjacent satellites with an overlapped coverage region, one satellite's coverage region should not contain the center point of the other satellite's coverage region. Otherwise, the stationary may not be optimal.

V. Distributed Coverage Control Synthesis

After receiving the target configuration $\mathbf{p}^{\mathrm{d}}$ from $(\mathcal{Q}_p)$, each satellite is controlled independently by solving the constrained-LQR problem $(\mathcal{Q}_{ci})$. Due to convex input constraints, we reformulate $(\mathcal{Q}_{ci})$ to the discrete counterpart and solve it efficiently. Let $\Delta t \in \mathbb{R}_+$ be the sampling period and $N = T_f/\Delta t$. We denote $p_{i,k} \in \mathbb{R}^2, v_{i,k} \in \mathbb{R}^2$, and $u_{i,k} \in \mathbb{R}^2$ as the position, velocity, and control thrusts of satellite S_i at time step k, $k = 0, 1, \ldots, N-1$. We write $q_{i,k} = [p_{i,k}^{\mathsf{T}} \ v_{i,k}^{\mathsf{T}}]^{\mathsf{T}} \in \mathbb{R}^4$, (A_d, B_d) as the corresponding discrete system dynamics of (4), and $\widetilde{Q}_i \in \mathbb{S}^{4\times 4}$ as the augmented weight matrix to penalize both position and velocity. Then, the discrete counterpart of $(\mathcal{Q}_{ci})$ can be written as

$$\begin{aligned} \min_{u_i} \quad & \left\|q_{i,N} - q_i^{\mathrm{d}}\right\|_{\widetilde{Q}_i}^2 + \sum_{k=0}^{N-1} \left\|q_{i,k} - q_i^{\mathrm{d}}\right\|_{\widetilde{Q}_i}^2 + \|u_{i,k}\|_{R_i}^2 \\ \text{s.t.} \quad & q_{i,k+1} = A_d q_{i,k} + B_d u_{i,k}, \quad k = 0, \ldots, N-1, \\ & u_{i,k}^{\mathsf{T}} u_{i,k} \leq (u_i^{\mathrm{m}})^2, \quad k = 0, \ldots, N-1. \end{aligned} \tag{$\widetilde{\mathcal{Q}}_{ci}$}$$

In practice, new attacks/incidents could happen during the satellite maneuver, causing further degeneration in the

coverage performance. To cope with these issues, we can set multiple waypoints along the trajectory to the target position. At each waypoint, the attack/incident detection is enabled so that satellites can readjust their controls to deal with the threats. More specifically, after receiving p_i^{d} from the DPGD algorithm, satellite S_i sets W_i waypoints $\{\widetilde{p}_i^{(m)}\}_{m=1}^{W_i}$ with $\widetilde{p}_i^{(W_i)} = p_i^{\mathrm{d}}$. If some satellite encounters a new attack/incident, the satellite goes to the nearest waypoint and restarts the DPGD algorithm to find another new configuration to adapt to the attack/incident.

We synthesize the DPGD planner and mwMPC controller into the following DPGD-mwMPC framework in Alg.2.

Algorithm 2: DPGD-mwMPC framework

1 **Initialize**: W_i for satellite S_i, $i = 1, \ldots, n$;
2 $\mathbf{p}^d \leftarrow$ DPGD planning algorithm (Alg. 1) ;
3 **for** *Satellite* $i = 1$ **to** n *(in parallel)* **do**
4 Receive p_i^{d} ;
5 Compute waypoints $\{\widetilde{p}_i^{(m)}\}_{m=1}^{W_i}$;
6 **for** $m = 1$ **to** W_i **do**
7 do MPC$(\widetilde{\mathcal{Q}}_{ci}^{(m)}, \widetilde{p}_i^{(m)})$;
8 **if** *new attack detected* **then**
9 **goto** DPGD planning algorithm (line 2);

MPC$(\widetilde{\mathcal{Q}}_{ci}^{(m)}, \widetilde{p}_i^{(m)})$ means performing MPC to satellite S_i based on the problem $\widetilde{\mathcal{Q}}_{ci}^{(m)}$ with the target position $\widetilde{p}_i^{(m)}$.

The DPGD-mwMPC framework enables a distributed and resilient approach for attacks and incidents that affect coverage performance. Each satellite can react to the new attack/incident in time by adjusting the number of waypoints. If the environment is secure enough, all satellites can simply set one waypoint during the maneuver. Otherwise, multiple waypoints can be set to monitor threats in real-time.

VI. Case Studies

In this section, we demonstrate the resiliency of our framework by considering cyber attacks on coverage operations. We consider a satellite constellation with $n = 25$ homogeneous LEO satellites. Each satellite has the same initial coverage parameters $(\alpha, \psi^{\mathrm{m}})$. We use normalized units as some parameters are huge such as the earth radius. We define 1 distance unit (DU) as 10^6m and 1 time unit (TU) as 10^2s (earth radius $R_e = 6.378$ DU). We set the orbital altitude $h = 800$km ($= 0.8$ DU) and FOV $= 48^\circ$, which are typical values for LEO satellites. The satellite period is $T_s = 6052.2$s ($= 6.052$ TU). The maximum control thrust for each satellite is assumed to be $T_{\max}/m = 0.01$ DU/TU^2 $:= u^{\mathrm{m}}$. We normalize the coverage intensities by setting $\psi^m = 10$ for all satellites. The demand intensity $\mu(\theta)$ is set as a truncated multimodal normal distribution on $[0, 2\pi)$ for the simulation purpose. The sampling period $\Delta t = 0.6$ TU and the control horizon $T_f = 18$ TU.

A. Coverage under Cyber Attacks

Cyber attacks such as jamming attacks can degenerate the coverage performance by reducing the FOV angle and the maximum coverage intensity ψ_i^{m}. Since cyber attacks generally do not destroy the physical equipment on satellites, the attacked satellite may recover to a certain extent after the attack is over. We consider the following attack-and-recovery plan where 6 satellites are attacked and then recovered. The attacked satellites' coverage parameters are changed according to Tab. I during and after the attack.

group #	satellite #	attack (FOV, ψ_i^m)	recovery (FOV, ψ_i^m)
group 1	1	$(44, 8)$	$(48, 10)$
	2	$(42, 7)$	$(47, 9)$
	3	$(42, 7)$	$(44, 8)$
group 2	19	$(44, 8)$	$(47, 9)$
	20	$(42, 6)$	$(45, 7)$
group 3	22	$(46, 8)$	$(48, 10)$

TABLE I: Attack and recovery plan.

The entire process is shown in Fig. 3a, and we divide it into three phases: initialization, attack, and recovery phases. In the initialization phase, all satellites find a local optimal configuration given the IC. The attack and the recovery phases show the reactions of the satellite constellation during and after the cyber attack, respectively. Three phases are distinguished by the jumps in the coverage cost, showing the destructiveness of the cyber attack to the coverage performance. Our framework shows resilient satellite control in all three phases. All satellites can not only adapt to the given initial configuration, but also mitigate the attack consequence and reduce the coverage cost. Eventually, a local optimal configuration is reached to adapt to the cyber attack. The zoomed plots show that all satellites actively seek to mitigate the attack and successfully improve coverage performance. In the recovery phase, the attack is over, and the attacked satellites recover partial coverage capability. Then all satellites readjust the configuration based on the recovered capabilities to provide better coverage performance.

We also experiment with full recovery by considering the same attack plan in Tab. I. The result is shown in Fig. 3b. We observe that the satellite constellation can still achieve the same coverage performance when the attack is over by using our framework. The zoomed plot successfully demonstrates the coverage performance converges to the pre-attack level.

We note that in all three phases, the coverage cost first drops fast and then slows down. It indicates that most satellites reach the target positions in a short time, and only a small portion of satellites require a longer time to maneuver due to limited mobility. Thus, we can use the DPGD-mwMPC framework to generate suboptimal configurations where some satellites only need to reach their intermediate waypoints. It is especially convenient when consecutive attacks happen. Besides, suboptimal configurations save more fuel (less control costs), implying that our framework can be used to balance the trade-off between the coverage performance and the fuel consumption.

B. Comparison with Equal-Spacing Control Strategy

We compare our algorithm with the equal-spacing control strategy, where all satellites aim to maintain an equal space in the configuration. We experiment with the constellation's

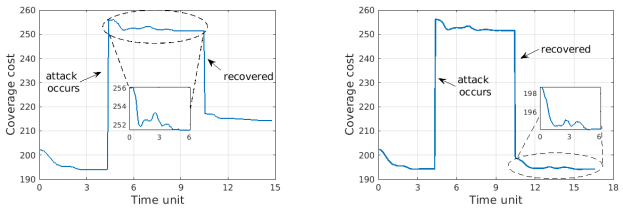

(a) Partial recovery. **(b)** Full recovery.

Fig. 3: Coverage cost evolution under cyber attacks.

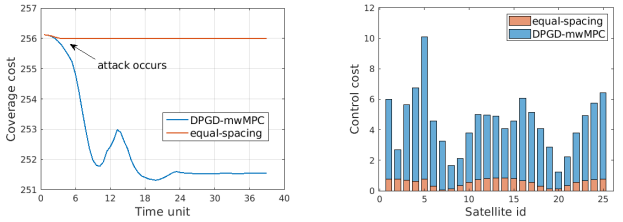

(a) Evolution of the coverage cost after the attack occurs. **(b)** Fuel consumption of each satellite.

Fig. 4: Comparison of DPGD-mwMPC framework and equal-spacing control under cyber attacks. We use the attack plan in Tab. I

reaction to the cyber attack in Tab. I by using the DPGD-mwMPC framework and the equal-spacing control strategy. The results are shown in Fig. 4a.

We observe that the equal-spacing control strategy has barely changed the coverage performance when the attack occurs, while the DPGD-mwMPC framework significantly reduces the coverage cost and improves the coverage performance. It shows that the equal-spacing strategy provides little resiliency in satellite coverage compared with our framework. We also plot the total control cost (representing fuel consumption) in Fig. 4b. It is clear that the DPGD-mwMPC framework requires more fuel to mitigate the attack and reach a better configuration, showing the trade-off between the coverage performance and the fuel consumption. However, the fuel consumption of our approach is not significantly greater than the one of equal-spacing control strategy. For some coverage-critical tasks such as battlefield communications, additional fuel consumption is tolerable. To save fuel, we can also steer satellites to some suboptimal configurations.

We mention that the equal-spacing control strategy is not effective for homogeneous satellite constellations because all satellites have the same spacing with adjacent satellites at the beginning. No matter what cyber attacks occur, all satellites simply remain in their original positions, showing zero resiliency and zero robustness.

VII. Conclusion

In this paper, we have investigated the satellite constellation coverage in a single orbit under adversarial environments by establishing a distributed and resilient planning-control framework. The proposed framework has not only captured the multi-objective of maximizing coverage performance and minimizing fuel consumption for satellite constellation readjustment, but also improved the resiliency of satellite constellation coverage for cyber attacks. The developed distributed algorithm has shown effectiveness in searching for optimal coverage configuration. The multi-waypoint MPC methodology has achieved fuel-optimal control. Case studies have demonstrated that the designed framework provides a strong resiliency to cyber attacks compared with the equal-spacing control strategy. For future work, we would consider the coordination and resilient control of multi-orbit satellite constellations. We would also investigate the impact of more sophisticated attacks on the satellite constellation coverage.

References

[1] G. Xu and Y. Xu, *GPS*. Springer, 2007.

[2] D. Roddy, *Satellite communications*. McGraw-Hill Education, 2006.

[3] J. B. Campbell and R. H. Wynne, *Introduction to remote sensing*. Guilford Press, 2011.

[4] Y. Ulybyshev, "Satellite constellation design for complex coverage," *Journal of Spacecraft and Rockets*, vol. 45, no. 4, pp. 843–849, 2008.

[5] H. W. Lee, S. Shimizu, S. Yoshikawa, and K. Ho, "Satellite constellation pattern optimization for complex regional coverage," *Journal of Spacecraft and Rockets*, vol. 57, no. 6, pp. 1309–1327, 2020.

[6] A. Al-Hourani, "Optimal satellite constellation altitude for maximal coverage," *IEEE Wireless Communications Letters*, 2021.

[7] J. G. Walker, "Satellite constellations," *Journal of the British Interplanetary Society*, vol. 37, p. 559, 1984.

[8] R. D. Luders, "Satellite networks for continuous zonal coverage," *ARS Journal*, vol. 31, no. 2, pp. 179–184, 1961.

[9] J. Hanson, M. Evans, and R. Turner, "Designing good partial coverage satellite constellations," in *Astrodynamics conference*, 1990, p. 2901.

[10] A. Al-Hourani, "An analytic approach for modeling the coverage performance of dense satellite networks," *IEEE Wireless Communications Letters*, vol. 10, no. 4, pp. 897–901, 2021.

[11] N. Okati, T. Riihonen, D. Korpi, I. Angervuori, and R. Wichman, "Downlink coverage and rate analysis of low earth orbit satellite constellations using stochastic geometry," *IEEE Transactions on Communications*, vol. 68, no. 8, pp. 5120–5134, 2020.

[12] T. Savitri, Y. Kim, S. Jo, and H. Bang, "Satellite constellation orbit design optimization with combined genetic algorithm and semianalytical approach," *International Journal of Aerospace Engineering*, vol. 2017, 2017.

[13] Z. Liu, C. Lin, and G. Chen, "Space attack technology overview," in *Journal of Physics: Conference Series*, vol. 1544, no. 1. IOP Publishing, 2020, p. 012178.

[14] B. Reiffen and H. Sherman, "Parametric analysis of jammed active satellite links," *IEEE Transactions on Communications Systems*, vol. 12, no. 1, pp. 102–103, 1964.

[15] H. Rausch, "Jamming commercial satellite communications during wartime an empirical study," in *Fourth IEEE International Workshop on Information Assurance (IWIA'06)*. IEEE, 2006, pp. 8–pp.

[16] M. Manulis, C. Bridges, R. Harrison, V. Sekar, and A. Davis, "Cyber security in new space: Analysis of threats, key enabling technologies and challenges," *International Journal of Information Security*, pp. 1–25, 2020.

[17] J. Chen and Q. Zhu, "Control of multilayer mobile autonomous systems in adversarial environments: A games-in-games approach," *IEEE Transactions on Control of Network Systems*, vol. 7, no. 3, pp. 1056–1068, 2019.

[18] J. Chen, C. Touati, and Q. Zhu, "A dynamic game approach to strategic design of secure and resilient infrastructure network," *IEEE Transactions on Information Forensics and Security*, vol. 15, pp. 462–474, 2019.

[19] Q. He and C. Han, "Dynamics and control of satellite formation flying based on relative orbit elements," in *AIAA Guidance, Navigation and Control Conference and Exhibit*, 2008, p. 6470.

[20] W. Clohessy and R. Wiltshire, "Terminal guidance system for satellite rendezvous," *Journal of the Aerospace Sciences*, vol. 27, no. 9, pp. 653–658, 1960.

[21] Y. Zhao and Q. Zhu, "Autonomous and resilient control for optimal leo satellite constellation coverage against space threats," *arXiv preprint arXiv:2203.02050*, 2022.